JOURNAL OF SOLID STATE CHEMISTRY **139,** 57–65 (1998)
ARTICLE NO. SC987807

Nonstoichiometry in Er–Te Binary and Er–Te–I Ternary Systems

K. Stöwe[1]

Institut für Anorganische Chemie und Analytische Chemie und Radiochemie, Saarbrücken, Saarland, Germany

Received October 27, 1997; in revised form February 23, 1998; accepted March 3, 1998

By X-ray single-crystal structure analysis of $Er_{0.85}Te$ and $Er_{17.3}Te_{24}I_8$, the structures of formerly unknown nonstoichiometric lanthanide tellurides could be solved and refined. Both structures may be derived from the cubic rock-salt type. As a result of vacancy ordering, the unit cell of the basic rock-salt type is doubled in all three directions [space group $Fd\bar{3}m$, $a = 1202.0(1)$ pm and $a = 1212.0(1)$ pm for $Er_{0.85}Te$ ($Z = 32$, $R_w = 4.64\%$) and $Er_{17.3}Te_{24}I_8$ ($R_w = 3.38\%$), respectively]. In both compounds, one of the two symmetrically equivalent cation sites is fully occupied by Er; the other is only partially occupied. Topologically, the cations of each partial structure are forming in the rock-salt type a framework of Er_4 tetrahedra sharing all corners. The diffraction pattern of the ternary compound can be interpreted only if a substitution of cations by tellurium ions is assumed giving a compound with polycationic and polyanionic structural fragments. The occurrence of these structural elements may be explained by assuming a partial overlap of Er-5d-and (Te, I)-5p-levels in the bandstructure.

INTRODUCTION

The largest group of nonstoichiometric compounds is that with a rock-salt-type structure. The homogeneity ranges of these compounds are the result of vacancies either in the cation or in the anion sublattice. The lattice parameters of this compound type are often quite insensitive to this drastic perturbation of stoichiometry [e.g., Er_2Te_3 (1)]. Frequently the vacancies are randomly distributed at high temperatures (above 1300–1500 K), but ordering occurs by annealing at lower temperatures. The transitions from a disordered to an ordered vacancy distribution are often very sluggish, and the high temperature polymorphs can readily be obtained by quenching. Despite the fact that the transition process in many cases obviously proceeds via first order, the Landau criteria for second-order transitions are frequently fulfilled. The resulting structure can be described by a supercell which is determined by a **k** vector of the first Brillouin zone of the basic rock-salt subcell. An ordering corresponding to all four vectors in the star of $\mathbf{k} = (\frac{1}{2}, \frac{1}{2}, \frac{1}{2})$ means a doubling of unit-cell dimensions in all three lattice directions. The vacancy ordering can be rather complex and need not be commensurate to the basic rock-salt subcell. Examples are $NbC_{0.83}$ and $VC_{0.83}$, which show a helical vacancy ordering pattern in the [111] direction (2, 3), or TaC_x ($x = 0.79$–0.9), which crystallizes with an incommensurate supercell (4).

Among the chalcogenides of 1 : 1 stoichiometry, the sulfides and selenides of groups 3 and 4 are the best-investigated systems (for a review see the survey in Ref. 5). Phases with defects in the chalcogenide sublattice commonly adopt the WC structure type in order to enhance metal–metal bonding as metal–chalcogen interactions diminish. In the metal-deficient phases, however, the structures with NaCl-type supercells dominate with partial or complete ordering of the vacancies. The corresponding tellurides do not seem to have extended homogeneity ranges, with the exception of $Zr_{1-x}Te$ with a defect NiAs-type structure ($x = 0$–0.5) (6). Nothing is explicitly reported in the literature about the occurrence of nonstoichiometric lanthanide tellurides.

Among the phases with a rock-salt supercell, the metal-deficient sulfides and selenides $M_{1-x}Q$ show only two different vacancy ordering arrangements in the range $0 < x < 0.3$. In the first arrangement, the vacancies order with a rhombohedral supercell in the space group $R\bar{3}m$. This variant can be regarded as a stuffed $CdCl_2$-type structure. The second arrangement is observed e.g., with the compound $Y_{0.78}Se$ (7), and it results in a doubling of the basic rock-salt subcell by ordering in the space group $Fd\bar{3}m$ (8, 9). Below the phase-transition temperature, superlattice reflections of half-numbered order appear in the diffraction pattern. These facts can be summarized by a group–subgroup relationship in the form of a "symmetry tree" according to Bärnighausen (10), which is illustrated by giving structural parameters:

[1]To whom correspondence should be addressed.

0022-4596/98 $25.00

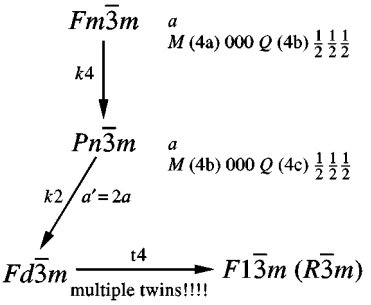

a'	$a'' = a\cdot\sqrt{2}$, $c'' = 2a\cdot\sqrt{3}$ (stuffed CdI_2-type)
M (16c) 0 0 0	M (3a) 0 0 0 M(9d) $\frac{1}{2}0\frac{1}{2}$
M (16d) $\frac{1}{2}\frac{1}{2}\frac{1}{2}$	M (3b) $00\frac{1}{2}$ M(9e) $\frac{1}{2}00$
Q (32e) $x\,x\,x\;x \sim \frac{1}{4}$	Q (6c) $00\,z\;z \sim \frac{1}{4}$
	Q (18h) $x\,\bar{x}\,z\;x \sim \frac{1}{2}$, $z \sim \frac{3}{4}$

Both transitions, $Fm\bar{3}m$ to $Fd\bar{3}m$ and $Fm\bar{3}m$ to $R\bar{3}m$, fulfill the Landau criteria with an ordering parameter $\mathbf{k} = (\frac{1}{2},\frac{1}{2},\frac{1}{2})$. However, as the symmetry tree indicates, the space group $R\bar{3}m$ is a maximal nonisomorphic subgroup of $Fd\bar{3}m$. Because the transition is *t*(*ranslationengleich*) (11), we have to expect the formation of multiple twin domains, each of which shows a deformation along one of the four originally equivalent $\langle 111\rangle$ directions. Thus, microtwinning complicates the distinction between the two types of vacancy arrangement. Unambiguous indications for a vacancy ordering in the rhombohedral space group are obtained only in the case of a significant deviation of the rhombohedral angle from the value $\cos^{-1}(5/6)$, which results in a splitting of the reflections at high Bragg angles in the diffraction pattern as for instance in $Zr_{1-x}S$ (5).

In the past, a number of publications tried to point out the relationship of electronic bandstructure effects to defect formation (12–14). On the other hand, models which argued on the basis of Madelung energies and configurational entropies, showed that coulombic forces did not lead to the observed ordering (15). Recently a model founded on self-consistent Linear Muffin-Tiu-Orbital (LMTO) bandstructure calculations was used by Burdett *et al.* to find out the origin of nonstoichiometry (5, 16, 17).

According to Burdett *et al.*, the stabilization of the MQ phases resulting from the loss of metallic component M on heating, which leads to the formation of the nonstoichiometric compound $M_{1-x}Q$, is the result of two different effects. By the removal of metal atoms, a part of the remaining ones increase their oxidation state from M^{2+} to M^{3+}. In this way, electrons from $M(d)$ bands formed by direct metal–metal interaction of the cations are removed. Because of the large intermetallic distances (see also Table 4) the covalent M–M interactions are only quite weak. As bandstructure calculations demonstrated (17), small amounts of chalcogen p-states mix with the metal d-levels. Especially in the upper half of the metallic d-bands, these states have a small M–Q antibonding character. Because of the electronic depletion of the d-bands not only is the Fermi level lowered, but the energy of the metallic d-states is also reduced. By lowering the energy, the loss of covalent M–M interaction resulting from oxidation is compensated to some extent. This first-order effect is schematically shown in Fig. 1. The energy lowering of the metal d-states brings the metal and chalcogen levels closer together so that their mutual interaction increases. This second-order effect leads to a stabilization of the states with largely chalcogen p-character (i.e., more tightly bound chalcogen atoms). If the effect is large enough, the energetic loss due to oxidation can be overcompensated, resulting in an overall stabilization of the nonstoichiometric phase in relation to the one with 1 : 1 stoichiometry. According to Burdett *et al.* (17), this model for the explanation of the origin of nonstoichiometry is not valid for compounds with a larger d-electron count like $Fe_{1-x}S$ or $Mn_{1-x}S$. In these compounds, the portion of the nonmetallic component in the $M(d)$-bands is larger, and the lowering of the energy by the oxidation from M^{2+} to M^{3+} smaller.

In the investigations which we will report here, we intended to examine the Ln–Te binary systems with respect to nonstoichiometric phases in the vicinity of the 1 : 1 composition. Beyond this, attention was also paid to the Ln–Te–I ternary systems, because Te^{2-} and I^- ions are of comparable size. As an example, the element erbium was chosen, but it is to be expected that several other lanthanide elements behave analogously. This was already verified with thullium, but systematic studies are yet missing.

Known phases in the Er–Te binary system (18) are ErTe and Er_2Te_3, and the phase diagram shows the formation of a solid solution between them. Additionally, the compound

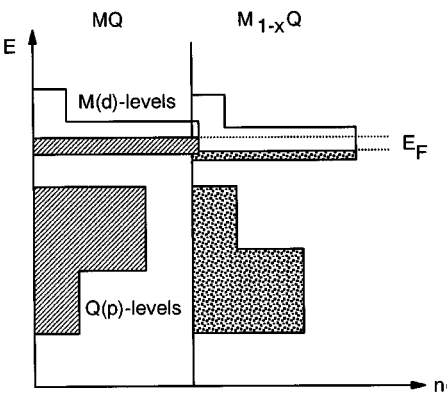

FIG. 1. Explanation of the origin of nonstoichiometry in the phases $M_{1-x}Q$ according to Burdett *et al.* (5, 16, 17). Effects of first and second order yield a stabilization of the compound on oxidation from M^{2+} to M^{3+}. Notice the energetic lowering of the $Q(p)$-levels according to the enlargement of the metal–chalcogen interaction.

$ErTe_3$ is found. It crystallizes, as the other lanthanide tritellurides, in the $NdTe_3$ structure type. ErTe itself crystallizes in the NaCl-type structure (19) and Er_2Te_3 in the so-called ζ- or Sc_2S_3-type of the lanthanide sesquichalcogenides (1, 20) which represents an ordered defect variant of the rock-salt type. The structural data of the compounds in the Er–Te binary system result from X-ray powder diffraction investigations (i.e., no data from single-crystal structure analysis were reported).

The *Ln–Q–X* ternary systems (X = Cl, Br, I) were intensively studied only for Q = S. Apart from 1 : 1 : 1 phases with the formula *LnSX*, notice is given of compounds of formula types such as $Ln_4S_3Br_6$ (Ln = La, Ce, Pr, Nd) (21, 22) and $Nd_3S_2Br_5$ (23). Compounds in the *Ln*–Te–*X* ternary systems (X = Cl, Br, I) are completely unknown in the literature.

EXPERIMENTAL

Sample Preparation

Erbium sesquitelluride Er_2Te_3, as a starting material for further synthesis, was prepared by chemical vapor transport reactions in sealed silica tubes with erbium trichloride as the transporting agent. By this method, single-crystals up to a size of 1.5 mm were grown. As starting materials for the transport reactions, we used powdered samples of the sesquitelluride prepared by annealing of the elements (Er: purity 99.9%, Kelpin; Te: purity > 99.999%, Fluka) in sealed silica tubes with Sigradur inlets at 1200°C for 3 days. These powders were subsequently transferred into the transport ampoules and ~30 mg of the transporting agent was added. The temperature gradient for vapor transport was 950°C → 800°C.

The erbium trihalides as transporting agents ($ErCl_3$) or starting materials for further synthesis of ternary compounds (ErI_3) were obtained by careful dehydration of the corresponding hydrates under high-vacuum conditions ($< 10^{-5}$ mbar) and subsequently purified by repeated sublimation in a silica tube with Ta inlet. The resulting sublimates were characterized by X-ray powder methods (Simon Guinier camera).

Single crystals of $Er_{1-x}Te$ were obtained by reaction of metallic Er with Er_2Te_3 single crystals in sealed silica tubes with Sigradur inlets and a loose lid by annealing at 850°C for 2 months. Synthesis of powdered samples was performed analogously by direct syntheses from the elements. To get samples annealed at higher temperatures (≥ 1200°C), these intermediate products were subsequently transferred into tantalum capsules, and the capsules were arc welded and held at a temperature of 1600°C by inductive heating. After 2 h, the temperature was lowered within 2 h and the samples annealed at the final temperature for 7 days.

All attempts to synthesize compounds of the formula $ErTe_xI_y$ by annealing directly mixtures of Er_2Te_3 and ErI_3 at temperatures up to 950°C failed, and the starting materials were regained unchanged. A reaction of the starting materials mentioned earlier is observed at 950°C only when metallic Er was added:

$$Er_2Te_3 + ErI_3 \not\rightleftharpoons 3ErTeI$$

$$xEr_2Te_3 + yErI_3 + (3 - 2x - y)Er \rightleftharpoons 3ErTe_xI_y$$

Because of the presence of ErI_3 with its noticeable vapor pressure at 950°C, a reaction with the silica tubes takes place with the formation of a disilicate with the formula $Er_2Si_2O_7$ (i.e., Er is removed from the equilibrium by this process). So additional Er has to be added.

All binary and ternary lanthanide compounds were handled under a dry and oxygen-free atmosphere of purified argon in a glove box because they were moisture- and air-sensitive.

Analytical Characterization

For a further characterization of the products with respect to their composition, atomic emission spectrometry with plasma excitation (ICP-OES, Perkin Elmer) was used. For analysis, the samples consisting of selected single crystals were sealed in capillaries of 2 mm diameter, subsequently opened in an autoclave with a Teflon inlet, and dissolved in a HNO_3/HCl mixture. Further details are given in Ref. 24.

To support the analytical data, the density of samples consisting of several single crystals were measured. This was done by a gas displacement pycnometer of type Accupyc 1330/1 cc (Micromeritics) with helium as working gas. In order to measure the density of the air- and moisture-sensitive samples, the complete pycnometer was placed in a glove box under a dried and oxygen-free argon atmosphere.

Additionally all products were characterized by X-ray powder diffraction methods (Simon Guinier camera). The refinement of the lattice parameters was done using 50 single-crystal reflections of uniform distribution in reciprocal space collected with a four-circle diffractometer (Siemens P4) with Eulerian cradle geometry and the computer program XSCANS (25). Structure solution and refinement were performed using the computer program package SHELXTL (26).

RESULTS AND DISCUSSION

Nonstoichiometry in the Er–Te System

To investigate the question whether there are nonstoichiometric phases in the Er–Te system and whether the

vacancies order in one of the previously mentioned arrangements, samples of different compositions in the range ErTe–Er_2Te_3 were prepared at several different temperatures and by different methods (see the experimental section). The obtained samples were examined by X-ray diffraction methods. The results can be summarized as follows.

Above 1200°C the two boundary phases in the range ErTe–Er_2Te_3 form a complete solid-solution series as already stated by Haase *et al.* (18). The diffraction pattern for samples liquefied in tantalum crucibles and annealed at temperatures ≥ 1200°C revealed the basic rock-salt subcell with $a_c = 606$ pm. The absence of any superstructure reflections indicates a statistical distribution of the vacancies. Below 1200°C, superstructure reflections which could be indexed by a cubic unit cell with eightfold cell volume (i.e., $a' = 2a_c$) appeared. The observed powder diffraction patterns of samples in the range ErTe–Er_2Te_3 resulted from the superposition of the individual diffraction patterns of the nonstoichiometric phase $Er_{1-x}Te$ and of the well-ordered compound Er_2Te_3.

In the compound ErTe, the formal Er^{2+} cation has the electron configuration [Xe] $4f^{11}5d^1$ i.e., the Er(*d*)-states are occupied with a single electron only (frequently written as $Er^{3+}(e^-)$ indicating an itinerant electron) and the prerequisite for the application of the model of Burdett (see introduction) is fulfilled. Theoretically the limit of the homogeneity range is reached at the composition $Er_{0.67}Te$ ($= Er_2Te_3$) where there are only Er^{3+} ions and unoccupied Er(5*d*)-bands. Practically this is only the case in the high-temperature polymorph. In this phase, a complete miscibility of the two boundary phases ErTe and Er_2Te_3 is observed. However, in the low-temperature polymorph below 1200°C with a partial ordering of the vacancy distribution, the field of existence of the nonstoichiometric phase does not extend up to $1 - x = 0.67$ because the X-ray diffraction patterns in the range $x = 0$–0.33 show two-phase mixtures consisting of the compounds $Er_{1-x}Te$ and Er_2Te_3. But because the unit cell parameters are rather insensitive against a variation of the vacancy concentration, we were not able to determine the homogeneity range x of the 1 : 1 boundary phase unambiguously.

Additionally by the topotactic reaction of metallic erbium with Er_2Te_3 crystals, which were prepared by a chemical vapor transport reaction, single crystals of the nonstoichiometric phase were grown by annealing the reaction mixtures at 850°C. On examination with a four circle diffractometer, these crystals also showed the superstructure reflections of the doubled rock-salt subcell. The analysis by ICP–OES yielded an averaged composition of $Er_{0.85(1)}Te$. The refinement of the structural parameters in the space group $Fd\bar{3}m$ with $a = 1202.0(1)$ pm indicated a partial occupation of the Er site (16*c*). From the X-ray analysis, a composition of $Er_{0.860(3)}Te$ resulted in agreement with the value determined by ICP–OES. A significant deviation of the unit-cell angles from 90° was not observed because the reflections did not split even for large Bragg angles 2θ. All attempts to refine structure models in the space groups $F\bar{4}3m$ (i.e., another subgroup of $Fd\bar{3}m$) and $Fm\bar{3}m$ (third possibility of vacancy ordering with $\mathbf{k} = (\frac{1}{2},\frac{1}{2},\frac{1}{2})$) yielded no improvements of the final *R*-values. This applies also for the refinement of the observed structure factor amplitudes in the space group $R\bar{3}m$ with the computer program package SHELXL-93 (27) under the assumption of a fourfold rotation-axis in one of the four equivalent [111] directions (regarding to the cubic supercell) as symmetry element for twinning in order to simulate the occurrence of twin domains with four different orientations. Tables 1–4 summarize important data collection parameters and refinement results of the structural parameters.

In the space group $Fd\bar{3}m$, the cation positions of the rock-salt lattice are divided into two equivalent partial structures of equal symmetry. Each of these partial structures forms topologically a framework of Er_4 tetrahedra

TABLE 1
Data Collection Parameters and Refinement Results of $Er_{0.860(3)}Te$

Measurement temperature		293 K
Unit-cell parameters	*a*	1202.0(1) pm
Number of formula units per cell		32
Calculated density		8.31(1) $g \cdot cm^{-3}$
Measured density		8.25(3) $g \cdot cm^{-3}$
Space group		$Fd\bar{3}m$ (No. 227)
Scan range (Mo$K\alpha$, entire sphere)		$3 < 2\theta < 70°$
Scan type and width		ω–2θ/1.0°θ in 96 steps
Number of observed reflections		8018
Number of independent reflections		331
Absorption correction method		numerical[a,b]
Crystal color		black
Crystal size		$\sim 0.24 \times 0.25 \times 0.24$ mm
Linear absorption coefficient		46.08 mm^{-1}
Internal *R*-value for averaging[c]		5.70%
Structure solution and refinement		SHELXTL PLUS[d]
Structure solution method		direct methods
Structure refinement method		full-matrix least-squares
Number of refined parameters		10
R-values [$W = 1/\sigma(F_0)^2$]		$R = 4.25\%$; $R_w = 4.64\%$

[a] W. Herrendorf, HABITUS, Program for the Optimization of the Crystal Description for a Numerical Absorption Correction on the Basis of Appropriate Psi-Scanned Reflections, Karlsruhe, Germany, 1992.

[b] N. W. Alcock, P. J. Marks, and K.-G. Adams, ABSPSI, Absorption Correction and Refinement of the Crystal Habitus, Karlsruhe, Germany, 1994.

[c] K.-G. Adams, MITTELN, Averaging Symmetry-Equivalent Reflections, Karlsruhe, Germany, 1995.

[d] SHELXTL PLUS, V.4.0, Program for Determination of Crystal Structures with X-Ray and Neutron Data, Siemens Analytical X-Ray Instruments, Inc., Madison, WI, 1990.

TABLE 2
Atomic Parameters and Equivalent Isotropic Displacement Parameters (in pm²) of $Er_{0.860(3)}Te$

Atom	Wyck.	x	y	z	s.o.f.	U_{eq}
Er(1)	16*c*	0	0	0	0.720(3)	84(2)
Er(2)	16*d*	0.5	0.5	0.5	1.0	92(1)
Te	32*e*	0.24817(2)	x	x	1.0	88(1)

Equivalent isotropic U calculated as a third of the trace of the orthogonal U_{ij} tensor.

TABLE 3
Anisotropic Displacement Parameters of $Er_{0.860(3)}Te$ (in pm²)

Atom	U_{11}	U_{22}	U_{33}	U_{23}	U_{13}	U_{12}
Er(1)	84(3)	U_{11}	U_{11}	4(2)	U_{23}	U_{23}
Er(2)	92(2)	U_{11}	U_{11}	3(2)	U_{23}	U_{23}
Te	88(2)	U_{11}	U_{11}	−4(2)	U_{23}	U_{23}

The exponent of anisotropic displacement parameter was used in the form:

$$-2\pi^2(h^2a^{*2}U_{11} + k^2b^{*2}U_{22} + l^2c^{*2}U_{33} + 2hka^*b^*U_{12} + 2hla^*c^*U_{13} + 2klb^*c^*U_{23}).$$

sharing all corners with an Er–Er distance of 424.95(2) pm. One of these partial structures is depicted in Fig. 2. Because only one site features vacancies, but the other one does not, the metallic conductivity of the 1 : 1 stoichiometry is preserved in the nonstoichiometric phase.[2]

Nonstoichiometry in the Ternary Er–Te–I System

The products resulting from the reactions of Er_2Te_3, ErI_3, and Er are green-black lustrous pieces of intergrown crystals. A corresponding Tm phase was prepared in the same way. According to X-ray diffraction data, both compounds crystallize in a face-centered cubic arrangement with $a = 1212.0(1)$ pm and $a = 1207.7(2)$ pm for the Er- and the Tm-compound, respectively. Both values were observed by refinement of the Bragg angles of single-crystal reflections collected with a four-circle diffractometer. Even though we were able to select single crystals of the Er compound, which revealed no indications for twinning on examination by a precession camera, no untwinned crystals of the corresponding Tm-phase were found. Because the elements tellurium and iodine cannot be distinguished by X-ray diffraction methods, the composition of the previously mentioned compounds had to be determined by analytical methods like ICP–OES. By atomic emission spectrometry, homogeneity ranges of $x = 1.2$–1.3 and $y = 0.3$–0.5 for the compounds with the general formula $Ln\mathrm{Te}_x\mathrm{I}_y$ (Ln = Er, Tm) were obtained. For the following explanations, a constant Te : I ratio of 3 : 1 was assumed, which is in accordance with the averaged composition of all investigated samples. To illustrate the nonstoichiometry of these phases in comparison to the rock-salt structure type, the notation as $Er_zTe_{24}I_8$ referring to an eightfold cell volume will be used in the following. For this ternary Er-phase single-crystal analysis also revealed the space group $Fd\bar{3}m$ with $2a_c$. The refinement of an analogous structure model as for $Er_{0.85}Te$ (two Er-sites of multiplicity 16, one with unrestricted occupation factor and an additional Te-site of multiplicity 32) gave a goodness of fit of $R = 6.25\%$ and $R_w = 5.32\%$ after numerical absorption correction and with anisotropic displacement factors. The composition resulting from the refinement of the X-ray data for this model was $Er(Te, I)_{1.20(1)}$ which deviates significantly from the value determined analytically. For this reason, this model was rejected.

The supercell reflections are much more intense in the compound $ErTe_xI_y$ than in $Er_{0.85}Te$. Therefore they allow a structure determination and refinement with substantially higher significance. A structure model for $ErTe_xI_y$ in accordance with the analytically determined composition can only be refined satisfactorally, if it is assumed that tellurium ions are situated at positions of erbium vacancies. The best R-values ($R = 2.73\%$ and $R_w = 3.36\%$) resulted from a model in which 25% of all Te ions of site (32*e*) are located at erbium positions of the partially occupied site (16*d*). By this, half of the site (16*d*) is occupied by anions. This ratio of the anions on the different lattice sites was held fixed during the subsequent refinements resulting from high correlations with several other parameters. Figure 3 gives a comparison of the theoretically calculated diffraction patterns for the different structure models with equal analytical composition: one with tellurium at erbium sites and the other one without. The calculation for the lower diagram in Fig. 3

TABLE 4
Selected Interatomic Distances Below 500 pm in $Er_{0.860(3)}Te$ (in pm)

Er(1)–Te distances:			Te–Te distances:		
Er(1)–Te	298.30(3)	6 ×	Te–Te	418.73(7)	3 ×
			Te–Te	424.98(2)	6 ×
Er(2)–Te distances:			Te–Te	431.17(7)	3 ×
Er(2)–Te	302.70(3)	6 ×	Er–Er distances:		
			Er(1)–Er(1)	424.95(2)	
			Er(1)–Er(2)	424.95(2)	
			Er(2)–Er(2)	424.95(2)	

[2] This was verified by measurement of the fundamental optical absorption which revealed no absorption edges in the range 15000–370 cm^{-1}.

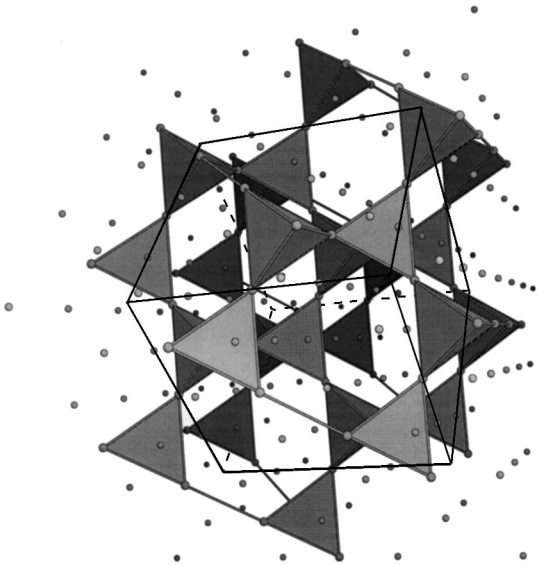

FIG. 2. Framework of all over corner-sharing Er_4 tetrahedra in $Er_{0.85}Te$ in a projection approximately in the direction of the space diagonal of the cubic unit cell. In the rock-salt structure type, two of these partial structures interpenetrate.

rests upon a model which was refined by means of the single-crystal data with tellurium at erbium sites. For the second one (upper diagram), the tellurium ions at the erbium lattice sites were simply removed, and the occupation number of the tellurium ions at the other site were raised by the same amount [R-values $R = 17.1\%$ and $R_w = 22.3\%$, U_{eq} of Er(2) not positive definite].

From the model with Te at Er positions a composition of $Er(Te, I)_{1.85(1)}$ or $Er_{17.3(1)}(Te, I)_{32}$ was derived by X-ray

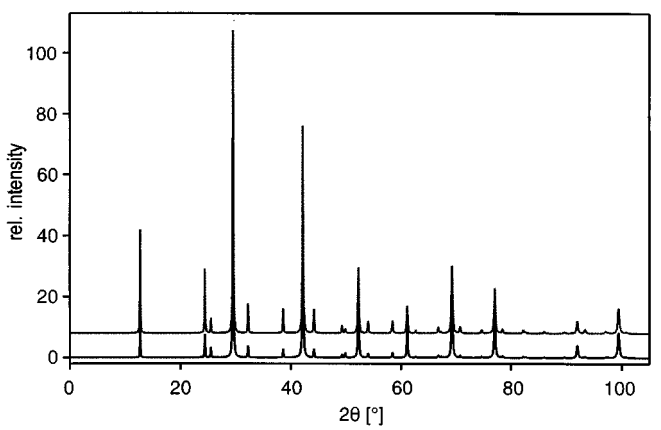

FIG. 3. Theoretical powder diffraction pattern for two different structure models of $ErTe_xI_y$. The calculation for the lower diagram rests upon a model with 25% of the tellurium atoms at erbium sites. The upper results under the assumption of a cation defect rock-salt-type structure with the same overall composition.

TABLE 5
Data Collection Parameters and Refinement Results of $Er_{17.3(2)}Te_{24}I_8$

Measurement temperature		293 K
Unit cell parameter	a	1212.0(1) pm
Number of formula unit per cell		32 "ErTe" units
Calculated density		6.50(1) $g \cdot cm^{-3}$
Measured density (see text)		6.58(2) $g \cdot cm^{-3}$
Space group		$Fd\bar{3}m$ (No. 227)
Scan range (Mo$K\alpha$, entire sphere)		$3 < 2\theta < 70°$
Scan type and width		ω–$2\theta/0.8°\theta$ in 96 steps
Number of observed reflections		8114
Number of independent reflections		221
Absorption correction		numerical[a,b]
Crystal color		black-green
Crystal size		$\sim 0.32 \times 0.24 \times 0.21$ mm
Linear absorption coefficient		33.21 mm^{-1}
Internal R-value for averaging[c]		9.58%
Structure solution and refinement		SHELXTL PLUS[d]
Structure solution method		direct methods
Structure refinement method		full-matrix least-squares
Number of refined parameters		11
R-values [$w = 1/\sigma(F_0)^2$]		$R = 2.73\%$; $R_w = 3.36\%$

[a] W. Herrendorf, HABITUS, Program for the Optimization of the Crystal Description for a Numerical Absorption Correction on the Basis of Appropriate Psi-Scanned Reflections, Karlsruhe, Germany 1992.

[b] N. W. Alcock, P. J. Marks, and K.-G. Adams, ABSPSI, Absorption Correction and Refinement of the Crystal Habitus, Karlsruhe, Germany, 1994.

[c] K.-G. Adams, MITTELN, Averaging Symmetry-Equivalent Reflections, Karlsruhe, Germany, 1995.

[d] SHELXTL PLUS, V.4.0, Program for Determination of Crystal Structures with X-Ray and Neutron Data, Siemens Analytical X-Ray Instruments, Inc., Madison, WI, 1990.

diffraction data analysis. By means of the analytically determined Te : I ratio, the formula of the compound can be written as $Er_{17.3(1)}Te_{24}I_8$. The derived structure model is not only in agreement with the analytical data, but also with those from density measurements (see Table 5). In this case, the measured density is a little bit larger than the theoretical one determined on the single crystal by X-ray diffraction. This is explained by the homogeneity range of the

TABLE 6
Atomic Parameters and Equivalent Isotropic Displacement Parameters (pm^2) of $Er_{17.3(2)}Te_{24}I_8$

Atom	Wyck.	x	y	z	s.o.f.	U_{eq}
Er(1)	16c	0	0	0	1.0	147(2)
Er(2)	16d	0.5	0.5	0.5	0.078(4)	112(2)
Te(1)	16d	0.5	0.5	0.5	0.5	$\equiv U_{eq}$(Er(2))
Te(2), I	32e	0.25044(3)	x	x	0.75	113(2)

Equivalent isotropic U calculated as a third of the trace of the orthogonal U_{ij} tensor.

TABLE 7
Anisotropic Displacement Parameters of $Er_{17.3(2)}Te_{24}I_8$ (in pm^2)

Atom	U_{11}	U_{22}	U_{33}	U_{23}	U_{13}	U_{12}
Er(1)	147(3)	U_{11}	U_{11}	−5(1)	U_{23}	U_{23}
Er(2)	112(4)	U_{11}	U_{11}	11(3)	U_{23}	U_{23}
Te(1)	$\equiv U_{11}$(Er(2))	U_{11}	U_{11}	$\equiv U_{23}$(Er(2))	U_{23}	U_{23}
Te(2), I	113(3)	U_{11}	U_{11}	−7(2)	U_{23}	U_{23}

The exponent of anisotropic displacement parameter was used in the form:

$$-2\pi^2(h^2a^{*2}U_{11} + k^2b^{*2}U_{22} + l^2c^{*2}U_{33} + 2hka^*b^*U_{12} + 2hla^*c^*U_{13} + 2klb^*c^*U_{23}).$$

compound and by the fact that another sample had to be chosen for the density measurements because the amounts were too small. The analytically determined composition of this sample is $ErTe_{1.31}I_{0.47}$, from which a density of $\rho = 6.60\,g\cdot cm^{-3}$ has to be calculated based on an unit-cell length of $a = 1212.2(1)$ pm as obtained by X-ray diffraction. Tables 5–8 summarize important refinement results.

Taking conventional formal oxidation states and assuming a Te : I ratio of 3 : 1 (i.e., the formula $Er_zTe_{24}I_8$) the value for z is calculated to 18.67. However, the analytically determined composition as well as the one determined by X-ray diffraction methods indicate a lower Er-content. This seems to be an additional clue to the occurrence of polytelluric structural fragments in this compound (Te at Er lattice sites i.e., in Te surrounding)). Regarding the difference of the ionic radii of Te^{2-} [$r(Te^{2-})^{[6]} = 221$ pm (28)] and Er^{3+} [$r(Er^{3+})^{[6]} = 89$ pm (28)], Te ions at Er lattice positions seem to be inconceivable at first sight. But in doing so, we have to keep in mind that the radii of polytelluric ions are considerably smaller than those of Te^{2-} ions. This may be illustrated by the layer structure of $U_{0.9}Te_3$ (29) where

TABLE 8
Selected Interatomic Distances Below 500 pm in $Er_{17.3(2)}Te_{24}I_{28}$ (in pm)

Er(1)–Te distances:		Te, I–Te, I distances:	
Er(1)–Te(2), I	303.53(4)	Te(1)–Te(2)	302.47(4)
		Te(2), I–Te(2), I	427.0(1)
Er(2)–Te, I distances:		Te(2), I–Te(2), I	428.50(2)
		Te(2), I–Te(2), I	430.0(1)
Er(2)–Te(2), I	302.47(4)		
Er–Er distances:			
Er(1)–Er(1)	428.50(2)		
Er(1)–Er(2), Te(1)	428.50(2)		
Er(2)–Er(2)	428.50(2)		

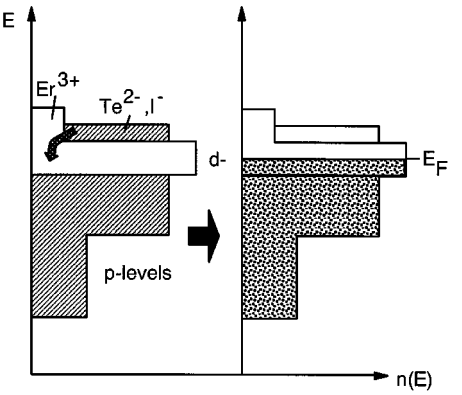

FIG. 4. Origin of the formation of polyanionic and polycationic structural fragments in the compound $ErTe_xI_y$. In the band structure Er($5d$)- and Te,I(p)-levels are schematically depicted.

4^4-nets consisting of Te^{2-} ions alternate with $(4^4)^2$-nets of Te^- ions packed with double density. In this compound, the relation $r(Te^-) = 1/2\sqrt{2}\cdot r(Te^{2-})$ holds. This demonstrates that a Te^- ion does indeed fit well into an octahedral void of Te^- ions[3]. The resulting Te–Te distances of 302.5 pm (see Table 8) are typical for polytelluric compounds with covalent tellurium bonds as the uranium tellurides (see, e.g. Ref. 24). Considering this, the observed Te : I ratio of 3 : 1 is highly plausible. In the compound $ErTe_xI_y$, there are iodide ions as well. But Te ions can only be inserted in voids solely built up from Te ions. Of the lattice site (32e), 75% is occupied by Te and 25% by I. Because only Te ions can be located at the Er positions of site (16d), 50% of the site (32e) is filled by Te, 25% by I, leaving 25% unoccupied. According to this, the average coordination number of the ions at the sites of multiplicity 16 is 4.5. This number may be calculated from integer coordination numbers lower than six only by the relation: $1/4\cdot(3\cdot 4 + 1\cdot 6) = 4.5$. At a Te : I ratio of 3 : 1 all Er ions of the lattice site (16c) as well as all Te ions of the site (16d) are surrounded by 4 Te ions. Together these amount to 3/4 of all "octahedral" voids. The remaining quarter of the octahedra must be built up from iodine ions. 16% of these ones are occupied by the remaining Er of the lattice site (16c) and about 84% remain unoccupied.

A close structural relationship between the compounds $Er_{0.85}$ Te and $ErTe_xI_y$ exists. In both phases an Er lattice site of multiplicity 16 is completely occupied (i.e., without vacancies). These erbium ions form a framework of Er_4 tetrahedra sharing all corners (see Fig. 2) and are responsible for metallic conductivity of the previously mentioned compounds.[3] But the conservation of the metallic conductivity in the depleted, nonstoichiometric compounds

[3] From another point of view, it is possible to argue that formally a Te^{4+} cation is sized [$r(Te^{4+})^{[6]} = 97$ pm (28)] to be suited in an octahedral void of Te^{2-} ions.

is possible only if one of the two equivalent Er-sites remains fully occupied.

Metallic conductivity requires free mobile electrons. In the compound $Er_{0.85}Te$ the unit cell formally contains $\sim 18.6\ Er^{2+}$ and $\sim 9.0\ Er^{3+}$ ions [i.e., 18.6 electrons per unit cell occupy the conduction band with predominantly Er(5*d*) character]. It is not possible to define an exactly analogous number in the compound in $ErTe_xI_y$ because the oxidation number of the tellurium ions is *a priori* not known. But by an exemplary calculation we want to illustrate in a short form how the presence of Te at Er positions can possibly lead to metallic conductivity despite the low erbium content (see earlier discussion). In Er_2Te_3 we simply have Er^{3+} and Te^{2-} ions, so the compound is a semiconductor. The erbium content in $ErTe_xI_y$ is still lower, but this phase seems to be a metallic conductor. As ^{125}Te–Moessbauer spectroscopy[4] revealed, the isomer shift of the tellurium ions in $ErTe_xI_y$ is comparable to that of the chain-forming $[Te^-]_2$ ions in the polytelluric compound UTe_3 (crystallizing in the $ZrSe_3$ structure type; see Ref. 24). When giving these a single negative charge (i.e., $U^{4+}Te^{2-}\ [Te^-]_2$), we would expect 19.8 electrons in the conduction band of $(Er^{3+})_{17.3(2)}(Te^-)_{24}(I^-)_8$. Because of the large intermetallic distances, the degree of covalent interaction is probably rather weak. The electrons necessary for charge balance may be delocalized in principle over the complete crystal, but a localization in form of cluster units may also be imagined. In this case, the framework of equally sized corner-sharing tetrahedra has to transform in a Peierl's distortion into one of reduced tetrahedral clusters with enforced M–M interactions alternating with enlarged tetrahedra without any intermetallic interactions ("breathing mode"). If clusters form, structural distortions will appear. Because twin domains will likely form (symmetry reduction from $Fd\bar{3}m$ to $F\bar{4}3m$), distortions will be recognizable only by enlarged temperature factors of Er. At ambient temperature, apparently nothing is detectable. But we have started to investigate whether a transition from itinerant to localized behavior will be observed at lower temperatures.

The occurrence of a compound with polycationic as well as polyanionic structural fragments is uncommon. Other examples of this phenomenon are compounds of type $(MSe_4)_nI$ (M = Nb, Ta and $n = 2, 3, 10/3$) (30–33), which contain one-dimensional metallic chains as well as Se_2 dumbbells as building units of the structure. At low temperatures, the formation of charge density waves (CDW) is observed in compounds of this type. Additionally the compound $Li_{12}Si_7$ and several other lithium silicides and germanides (34) have to be mentioned, in which polyanions (Zintl anions) and polycations (clusters) exist at the same time. To explain the simultaneous occurrence of polyanionic and polycationic structural fragments in the compound $ErTe_xI_y$, we propose the following model, which is founded on the schematic presentation of the electronic bandstructure for nonstoichiometric chalcogenides of the type $M_{1-x}Q$ as already given in Fig. 1.

In the tellurides, the energetic difference between the metal *d*-bands and the $Q(p)$-states is smaller than in the other chalcogenides (Q = S, Se). It is conceivable that because of the presence of iodine atoms in $ErTe_xI_y$, a situation with a mutual overlap of cationic *d*- and anionic *p*-levels occurs (see Fig. 4). If only Er^{3+} and Te^{2-} ions were present in the crystal structure, like in the compound Er_2Te_3, the Er(5*d*)-levels would be entirely unoccupied and the Te,I(*p*)-levels would be entirely filled (i.e., the compound would be a semiconductor). Because of the lowering of the bottom of the cationic *d*-bands below the upper edge of the anionic *p*-bands, a transition of electrons from *p*- to *d*-states is observed, equivalent to the occurrence of an internal redox-process. As a consequence, the formation of polycationic and polyanionic structural fragments is observed. A comparable situation is found, for instance, in the metallic compound $TiTe_2$ with a CdI_2-type structure, but without an interchange of anionic and cationic lattice positions. Instead merely the Te–Te distances are shortened to 377 pm in $TiTe_2$ (35). Additionally in several other compounds of the CdI_2-type [e.g., in ReS_2 (36) or in VTe_2 (37), a clustering of the metal atoms within the cation layers in a rather complex way is found.

[4] We will report the results of the ^{125}Te–Moessbauer spectroscopic investigation separately.

ACKNOWLEDGMENT

We gratefully acknowledge the financial support of the Fond der Chemischen Industrie.

REFERENCES

1. K. Stöwe, *Z. Anorg. Allg. Chem.*, **624,** 872 (1998).
2. A. I. Gusev and A. A. Rempel, *Phys. Status Solidi* **93,** 71 (1986).
3. J. Billingham, P. S. Bell, and M. H. Lewis, *Acta Crystallogr.* **A28,** 602 (1972).
4. A. A. Rempel, V. W. Lipatnikov, and A. I. Gusev, *Dokl. Akad. Nauk SSSR* **310,** 878 (1990).
5. J. K. Burdett and J. F. Mitchell, *Prog. Solid State Chem.* **23,** 131 (1995).
6. H. Sodeck, H. Mikler, and K. L. Komarek, *Monat. Chem.* **110,** 1 (1979).
7. S.-J. Kim and H. F. Franzen, *J. Less-Common Met.* **144,** 117 (1988).
8. H. F. Franzen, "Physical Chemistry of Inorganic Crystalline Solids," p. 121. Springer Verlag, Berlin, 1986.
9. H. F. Franzen, *Chem. Mater.* **2,** 486 (1990).
10. H. Bärnighausen, *MATCH*, *Communications in Mathematical Chemistry* **9,** 139 (1980).
11. "International Tables for Crystallography," vol. A (T. Hahn, Ed.). Reidel Publishing Company, Dordrecht (Holland) and Boston (USA), 1983.
12. H. F. Franzen, J. F. Nakahara, and D. K. Misemer, *J. Solid State Chem.* **61,** 338 (1986).
13. D. K. Misemer and J. F. Nakhara, *J. Chem. Phys.* **80,** 1964 (1984).

14. S. P. Denker, *J. Less-Common Met.* **14,** 1 (1968).
15. H. F. Franzen and J. A. Merrick, *J. Solid State Chem.* **33,** 371 (1980).
16. J. K. Burdett and J. F. Mitchell, *Chem. Mater.* **5,** 1465 (1993).
17. J. K. Burdett, S. C. Sevov, and O. Mryasov, *J. Phys. Chem.* **99,** 2696 (1995).
18. D. J. Haase, H. Steinfink, and E. Weiss, *J. Inorg. Chem.* **4,** 541 (1965).
19. L. H. Brixner, *J. Inorg. Nucl. Chem.* **15,** 199 (1960).
20. J. Flahaut, L. Domange, M. Guittard, M. Pardo, and M. Patrie, *C. R. Acad. Sci.* **257,** 1530 (1963).
21. C. Dragon and F. Thevet, *Ann. Chim. Fr.* **5,** 585 (1980).
22. N. Rysanek, A. Mazurier, P. Laruelle, and C. Dragon, *Acta Crystallogr.* **B36,** 2930 (1980).
23. M. Julien-Pouzol, S. Jaulmes, P. Laruelle, and C. Dragon, *Acta Crystallogr.* **C41,** 1286 (1985).
24. K. Stöwe, *Z. Anorg. Allg. Chem.* **622,** 1419 (1996).
25. XSCANS, V.2.1, X-Ray Single Crystal Analysis Software, Siemens Analytical X-Ray Instruments, Inc., Madison, WI 1994.
26. SHELXTL PLUS, V.4.O, Program for the Determination of Crystal Structures from X-Ray and Neutron Diffraction Data, Siemens Analytical X-Ray Instruments, Inc., Madison, WI 1990.
27. G. M. Sheldrick, SHELXL-93, FORTRAN-77 Program for the Refinement of Crystal Structures from Diffraction Data, Göttingen, 1994; G. M. Sheldrick, *Acta Crystallogr.* **A46,** 467 (1990).
28. R. D. Shannon, *Acta Crystallogr.* **A32,** 751 (1976).
29. K. Stöwe, *Z. Anorg. Allg. Chem.* **623,** 749 (1997).
30. A. Meerschaut, P. Palvadeau, and J. Rouxel, *J. Solid State Chem.* **20,** 21 (1977).
31. A. Meerschaut, P. Gressier, L. Guemas, and J. Rouxel, *J. Solid State Chem.* **51,** 307 (1984).
32. P. Gressier, L. Guemas, and A. Meerschaut, *Mat. Res. Bull.* **20,** 539 (1985).
33. B. Dardel, D. Malterre, M. Grioni, P. Weibel, Y. Baer, and F. Lévy, *Phys. Rev. Lett.* **67,** 3144 (1991).
34. R. Nesper, thesis for the certification of habilitation, p. 19, Stuttgart 1988.
35. J. Rouxel, *Chem. Eur. J.* **2,** 1053 (1996).
36. J. C. Wilderwanck and F. Jellinek, *J. Less-Common Met.* **24,** 73 (1971).
37. E. Canadell, S. Jobic, R. Brec, J. Rouxel, and M.-H. Whangbo, *J. Solid State Chem.* **99,** 189 (1992).